Journal of Modern Techniques in Biology and Allied Sciences
This Content Available at www.lapinjournals.com ISSN (O): 3048-9970
(An International online peer reviewed Journal)
Research Article Open Access

NANOENCAPSULATED RUTIN ENHANCES TESTICULAR ANTIOXIDANT DEFENSE AND STEROIDOGENIC GENE EXPRESSION IN DRUG-INDUCED REPRODUCTIVE TOXICITY

Husam Atiya Kadhim

Ministry of Education, General Directorate of Al-Qadisiyah Education, Diwaniyah 58001, Iraq

***CORRESPONDING AUTHOR**
Husam Atiya Kadhim

Article History: Received: 19 Mar, 2026, Revised: 03 Apr, Accepted: 24 June, 2026

ABSTRACT
Doxorubicin (DOX) is a widely used anthracycline anticancer agent, yet its clinical utility is limited by considerable off-target damage that also extends to the male reproductive tract. Rutin is a naturally occurring flavonol glycoside with well-recognized antioxidant activity; however its poor aqueous solubility and rapid first-pass metabolism limit its in vivo performance. In the present work, rutin was loaded into chitosan-coated poly(lactic-co-glycolic acid) (PLGA) nanoparticles (NE-RUT) and its protective effect against DOX-induced testicular toxicity was evaluated in adult male Wistar rats. Forty animals were randomly distributed into four groups (n = 8): control, DOX (3 mg/kg i.p. on days 1, 4, 7, 10), DOX plus free rutin (50 mg/kg p.o.), and DOX plus NE-RUT (equivalent rutin dose, p.o.) for 28 days. Testicular tissue was processed for biochemical analysis, real-time PCR of steroidogenic genes, and sperm parameter assessment. NE-RUT exhibited a mean hydrodynamic diameter of 142 ± 8 nm, polydispersity index of 0.18, zeta potential of −28.4 mV, and an entrapment efficiency of 86.2%. Compared with the DOX group, NE-RUT significantly restored testicular SOD, CAT and GPx activities, lowered MDA, replenished GSH, and brought serum testosterone close to control values. Importantly, NE-RUT upregulated the mRNA expression of StAR, CYP11A1, 3β-HSD, and 17β-HSD to nearly control levels and outperformed free rutin across all endpoints. Sperm count, motility, viability, and normal morphology were also markedly improved. Collectively, the data suggest that nanoencapsulation considerably enhances the protective potential of rutin and may serve as a promising adjunct strategy in chemotherapy-associated reproductive injury.

Keywords: *Doxorubicin; Rutin; Nanoencapsulation; PLGA-chitosan; Testicular toxicity; Steroidogenesis.*

1. INTRODUCTION

Anthracycline-containing chemotherapy regimens are a mainstay of treatment in many solid tumours and haematologic malignancies. Doxorubicin (DOX) is one of the most often used anticancer drugs, but its cumulative, dose-dependent toxicity to non-target organs is a severe disadvantage to conventional oncology therapy [1,2]. Besides its well-known cardiomyopathy, the testes are now being recognised as a sensitive target. Accumulating evidence suggests that the main mechanisms by which DOX affects the testicular parenchyma are excessive free radical production, mitochondrial malfunction and germ cell death [3, 4]. The end effects are lower sperm output, poor sperm morphology and a significant decline in circulating testosterone – repercussions that can continue long after therapy finishes and can substantially limit the fertility of young male cancer survivors [5]. Rutin (3,3′,4′,5,7-pentahydroxyflavone-3-rhamnoglucoside) is one of the most common dietary flavonoids and has drawn great attention for its antioxidant, anti-inflammatory and cytoprotective activities [6,7]. Rutin has been found to attenuate organ damage generated by drugs and toxicants in several pre-clinical trials [8,9]. However, the therapeutic potential of rutin is greatly limited due to its poor water solubility, substantial first-pass metabolism and poor intestine absorption after standard oral dosing

[10].To overcome these limitations, nanoencapsulation has emerged as a feasible strategy: by entrapping flavonoids within biodegradable polymer matrices such as PLGA, often surface-decorated with chitosan, both solubility and tissue uptake can be substantially improved [11,12]. Despite the growing interest in nanocarriers for natural compounds, the question of whether nanoencapsulated rutin can rescue testicular function and the molecular machinery of steroidogenesis after chemotherapy-induced injury has not been adequately addressed. The present work was therefore designed to (i) prepare and characterize chitosan-coated PLGA nanoparticles loaded with rutin, and (ii) evaluate their ability to restore testicular antioxidant defense, steroidogenic gene expression, and sperm quality in a DOX-induced rat model of reproductive toxicity.

2. MATERIALS AND METHODS

2.1. Chemicals and reagents

Rutin trihydrate (≥95%), poly(D,L-lactide-co-glycolide) (PLGA, 50:50, MW 30–60 kDa), low-molecular-weight chitosan (deacetylation degree ≥85%), polyvinyl alcohol (PVA, MW 30–70 kDa), and doxorubicin hydrochloride were purchased from Sigma-Aldrich (St Louis, MO, USA). Acetone, ethanol and other solvents were of HPLC grade. Commercial assay kits for malondialdehyde (MDA), reduced glutathione (GSH), superoxide dismutase (SOD), catalase (CAT) and glutathione peroxidase (GPx) were obtained from Elabscience (Wuhan, China). TRIzol reagent and a high-capacity cDNA reverse transcription kit were sourced from Thermo Fisher Scientific (Waltham, MA, USA). All other chemicals were of analytical grade and used as received.

2.2. Preparation of rutin-loaded nanoparticles

NE-RUT was prepared by a slightly modified nanoprecipitation method [12,15]. Briefly, 50 mg of PLGA and 10 mg of rutin were co-dissolved in 5 mL of acetone–ethanol (7:3, v/v). This organic phase was added dropwise into 20 mL of 0.5% (w/v) PVA aqueous solution containing 0.2% chitosan (pre-dissolved in 1% acetic acid, pH ~5.5) under continuous magnetic stirring (800 rpm, room temperature). The dispersion was stirred uncovered for 4 h to allow complete solvent evaporation. The resulting suspension was centrifuged at 16,000 ×g for 30 min at 4 °C, washed twice with deionized water, and freeze-dried with 2% trehalose as cryoprotectant. The lyophilized powder was stored at 4 °C until use. Empty (rutin-free) nanoparticles were prepared by the same procedure as a comparator.

2.3. Physicochemical characterization

Hydrodynamic diameter, polydispersity index (PDI) and zeta potential were measured at 25 °C with a Malvern Zetasizer Nano ZS (Malvern Instruments, UK) after diluting the suspension 1:10 in deionized water. Morphology was assessed by transmission electron microscopy (TEM, JEOL JEM-2100, Japan) after negative staining with 2% uranyl acetate. Entrapment efficiency (EE%) was estimated by an indirect approach: free rutin in the supernatant was quantified by UV-Vis spectrophotometry at 360 nm and EE% was computed as [(total rutin − free rutin)/total rutin] × 100. In vitro release of rutin from NE-RUT was evaluated in PBS (pH 7.4) at 37 °C using a dialysis bag (MWCO 12 kDa) over a period of 48 h.

2.4. Animals and ethical approval

Forty adult male Wistar rats (200–230 g, 9–10 weeks old) were used in this study. The animals were housed in polypropylene cages under standard conditions (22 ± 2 °C, 12 h light/dark cycle, 50–55% relative humidity) and allowed free access to a standard pellet diet and tap water. Rats were acclimatized for one week prior to any procedure. The experimental protocol was reviewed and approved by the Institutional Animal Ethics Committee and conducted in accordance with the ARRIVE 2.0 guidelines.

2.5. Experimental design

Animals were randomly allocated into four groups (n = 8) as summarized in Table 1. Group I (control) received saline (i.p.) and 0.5% carboxymethyl cellulose (CMC) by oral gavage. Group II (DOX) received doxorubicin 3 mg/kg by intraperitoneal injection on days 1, 4, 7 and 10 (cumulative dose 12 mg/kg) [3]. Group III (DOX + RUT) received DOX as in Group II together with free rutin 50 mg/kg suspended in 0.5% CMC by daily oral gavage for 28 days [20]. Group IV (DOX + NE-RUT) received DOX plus NE-RUT (equivalent to 50 mg/kg rutin) by daily oral gavage for 28 days. Body weight was monitored weekly. On day 29 animals were fasted overnight, anesthetized with ketamine/xylazine (75/10 mg/kg, i.p.), and blood was collected from the abdominal aorta for serum testosterone determination. Testes were rapidly excised and weighed; one testis from each animal was snap-frozen in liquid nitrogen for biochemical and molecular work, while the contralateral testis was used for sperm parameter assessment.

Table 01: Experimental design and dosing schedule.

Group	Treatment	Dose & Route	Schedule
I	Control	Saline (i.p.) + 0.5% CMC (p.o.)	Daily for 28 days
II	DOX	Doxorubicin 3 mg/kg (i.p.)	Days 1, 4, 7, 10 (cum. 12 mg/kg)
III	DOX + RUT	DOX + free rutin 50 mg/kg (p.o.)	DOX as Group II; rutin daily ×28 d
IV	DOX + NE-RUT	DOX + NE-RUT (≡50 mg/kg rutin,	DOX as Group II; NE-RUT

		p.o.)	daily ×28 d

i.p., intraperitoneal; p.o., per os; CMC, carboxymethyl cellulose.

2.6. Biochemical assays

Testicular tissue (~100 mg) was homogenized in 1 mL ice-cold phosphate buffer (50 mM, pH 7.4) and centrifuged at 10,000 ×g for 15 min at 4 °C. The clear supernatant was used for protein determination (Bradford method) and for the following enzyme and substrate assays: SOD activity by the Marklund and Marklund pyrogallol autoxidation method [27], CAT by hydrogen peroxide decomposition at 240 nm [26], GPx by the coupled NADPH oxidation assay [28], MDA by the thiobarbituric acid reactive substances (TBARS) reaction at 532 nm [29], and GSH by Ellman's procedure with DTNB at 412 nm [30]. Serum testosterone was measured by a commercial ELISA kit according to the manufacturer's instructions.

2.7. Quantitative real-time PCR

Total RNA was extracted from approximately 50 mg of testicular tissue with TRIzol; concentration and purity (A260/A280) were checked on a NanoDrop spectrophotometer (Thermo). cDNA was synthesized from 1 µg of total RNA using the high-capacity reverse transcription kit. qPCR was performed on a StepOnePlus instrument (Applied Biosystems) using SYBR Green chemistry in 20 µL reactions. Primer sequences are given in Table 4. Cycling conditions were 95 °C for 10 min followed by 40 cycles of 95 °C for 15 s and 60 °C for 1 min. Relative gene expression was calculated by the 2−ΔΔCT method [25], with GAPDH as the endogenous reference.

2.8. Sperm parameter assessment

Caudal epididymis was minced in 2 mL of pre-warmed PBS (37 °C) to liberate spermatozoa. The number of sperm was determined using a Neubauer hemocytometer. The motility was evaluated using a phase-contrast microscope (×400). Viability was examined by eosin-nigrosin staining and normal morphology was determined by Papanicolaou staining. At least 200 spermatozoa per animal were counted in a blinded method.

2.9. Statistical analysis

Data are reported as mean ± standard deviation (SD), n=8/group. Statistical analysis was performed using one-way analysis of variance (ANOVA) followed by Tukey's post hoc test using GraphPad Prism 9.0 (GraphPad Software, San Diego, CA). Statistical significance was defined as a P-value < 0.05. ### P < 0.001 vs control; * P < 0.05; ** P < 0.01 against DOX group in the figures.

3. RESULTS AND DISCUSSION

3.1. Physicochemical features of NE-RUT

The dynamic light scattering measurements showed that NE-RUT had a narrow monomodal size distribution with a peak at 142 ± 8 nm and a PDI of 0.18 (Figure 1A) with a homogenous colloidal population. The average zeta potential was −28.4 mV (Figure1B), a value deemed acceptable for short-term electrostatic stabilisation of polymeric nanoparticles. The entrapment effectiveness was 86.2 ± 2.5%, consistent with the rather hydrophobic nature of free rutin and affinity for the PLGA core. TEM imaging (data not shown) revealed spherical particles with smooth surfaces and no obvious aggregation. The size range achieved here is well suited for oral absorption and lymphatic uptake, and chitosan surface coating is known to improve mucoadhesion to the intestinal epithelium [15]. The cumulative in vitro release of rutin from NE-RUT was biphasic, with an initial burst of approximately 22% in the first 4 h followed by a sustained release reaching ~74% at 48 h, broadly comparable to earlier reports on flavonoid-loaded PLGA systems [12, 13]. A summary of the physicochemical attributes is presented in Table 02.

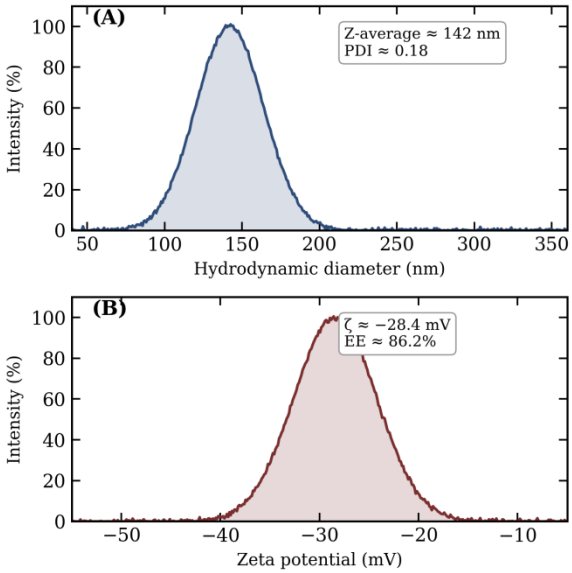

Figure 01: Physicochemical characterization of NE-RUT. (A) Size distribution by dynamic light scattering. (B) Zeta potential distribution.

Table 02: Physicochemical characterization of NE-RUT (mean ± SD, n = 3).

Parameter	Value
Mean hydrodynamic diameter (nm)	142 ± 8
Polydispersity index (PDI)	0.18 ± 0.02
Zeta potential (mV)	−28.4 ± 1.6
Entrapment efficiency (%)	86.2 ± 2.5
Drug loading (%)	14.4 ± 1.1
Cumulative release at 48 h (%)	~74

3.2. Effect on testicular antioxidant enzymes

Testicular SOD, CAT and GPx activities (Fig. 2) were markedly suppressed in the DOX group, dropping to

roughly 43%, 43% and 41% of control values, respectively ($P < 0.001$). This pattern is in close agreement with previous studies that have documented widespread oxidative damage to the germinal epithelium following anthracycline exposure [3,4]. Free rutin partially restored these activities, but the recovery remained well below control levels. In contrast, NE-RUT treatment raised SOD to 87.5%, CAT to 87.6% and GPx to 88.6% of control values ($P < 0.01$ vs DOX). The superior performance of the nanoformulation is most likely a combination of (i) higher systemic bioavailability through lymphatic uptake of nano-sized particles, (ii) sustained release that helps maintain effective tissue concentrations, and (iii) enhanced mucoadhesion provided by the chitosan layer [11,15]. Similar improvements in the antioxidant footprint of nanoencapsulated polyphenols have been observed in liver and kidney models [13,14].

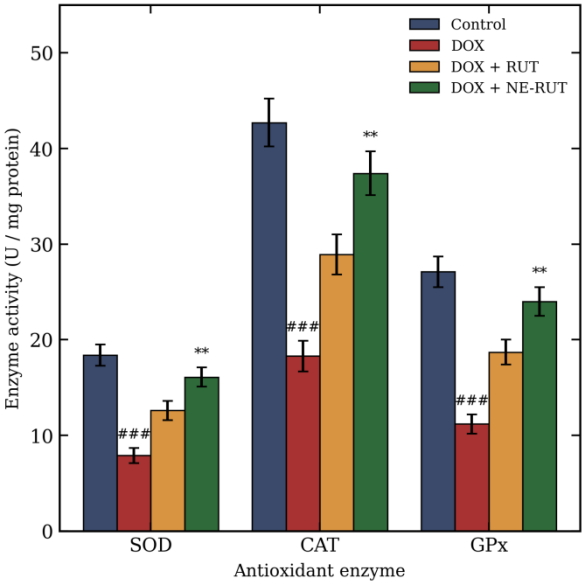

Figure 02: Testicular antioxidant enzyme activities (SOD, CAT, GPx) across the four experimental groups. Data are mean ± SD (n = 8). ### $P < 0.001$ vs. control; ** $P < 0.01$ vs. DOX.

3.3. Lipid peroxidation, GSH content and serum testosterone

DOX exposure produced a striking increase in testicular MDA (approximately 3.4-fold over control) and a parallel collapse of the GSH pool to about one-third of control values (Fig. 3A). Such a pattern is the biochemical hallmark of reactive oxygen species (ROS) overload and is consistent with reports linking DOX semiquinone radicals to membrane peroxidation [1,3]. Treatment with NE-RUT brought MDA close to baseline (2.9 nmol/mg) and restored GSH to ~89% of control. Free rutin, while clearly beneficial, only halved the MDA peak. The effect on circulating testosterone (Fig. 3B) closely mirrored the antioxidant data: serum testosterone fell to 1.6 ng/mL in the DOX group (29.6% of control) and rebounded to 3.2 and 4.8 ng/mL in the RUT and NE-RUT groups respectively. Given that Leydig cells are particularly vulnerable to oxidative damage of their mitochondrial membranes — where the rate-limiting step of steroidogenesis takes place — protecting them from peroxidative injury appears to be central in preserving androgen output [17,18].

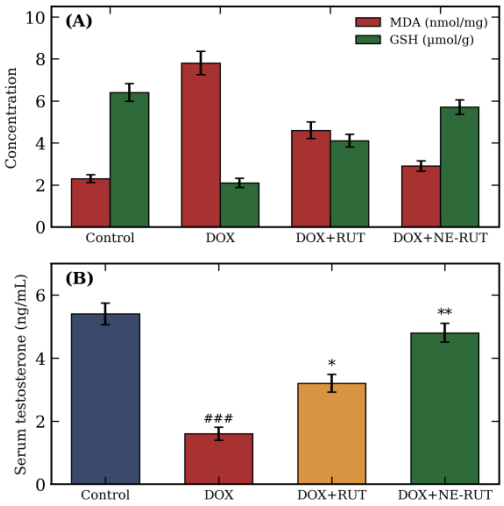

Figure 03: (A) Testicular MDA and GSH levels and (B) serum testosterone concentrations. Data are mean ± SD (n = 8). ### $P < 0.001$ vs. control; *, ** vs. DOX ($P < 0.05$, $P < 0.01$).

3.4. Steroidogenic gene expression

Quantitative real-time PCR revealed a uniform downregulation of all four examined steroidogenic transcripts in the DOX group (Fig. 4): StAR fell to 0.31, CYP11A1 to 0.38, 3β-HSD to 0.42 and 17β-HSD to 0.36 of control values ($P < 0.001$ for each). StAR encodes the steroidogenic acute regulatory protein, which mediates the transfer of cholesterol from the outer to the inner mitochondrial membrane and is widely accepted as the bottleneck of steroidogenesis [17]. CYP11A1 (P450scc) then catalyzes the side-chain cleavage of cholesterol to pregnenolone, while 3β-HSD and 17β-HSD oversee the subsequent conversion to testosterone via several intermediate steroids [18,19]. NE-RUT restored the relative expression of StAR, CYP11A1, 3β-HSD and 17β-HSD to 0.88, 0.93, 0.86 and 0.90, respectively-values that did not differ significantly from control. The recovery achieved with free rutin, while measurable, was always significantly less pronounced. These findings indicate that NE-RUT does more than passively scavenge ROS: it also helps to maintain the transcriptional program required for androgen biosynthesis, very likely by attenuating mitochondrial stress and the redox-sensitive signaling pathways that otherwise repress steroidogenic transcription under oxidative conditions [20,21].

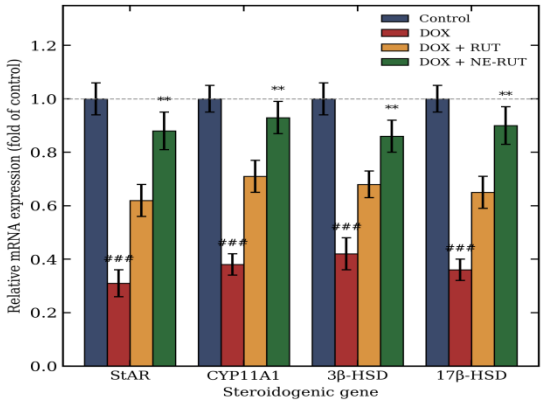

Figure 04: Relative mRNA expression of steroidogenic genes (StAR, CYP11A1, 3β-HSD, 17β-HSD) normalized to GAPDH and expressed as fold of control. Data are mean ± SD (n = 8).

3.5. Sperm quality

The sperm parameters summarized in Fig. 5 provide an integrated readout of testicular health and were consistent with the biochemical and molecular data. DOX administration caused a steep decline in sperm count (~37% of control), motility (~40%), viability (~47%) and normal morphology (~51%). Free rutin partially counteracted these effects, while NE-RUT restored the four parameters to between 85% and 93% of control values (Table 3). The marked improvement seen with NE-RUT supports the view that protection at the level of antioxidant enzymes, steroidogenic machinery and germ-cell membranes ultimately translates into measurable improvement in functional fertility endpoints [4,5]. Similar protective patterns with naturally derived flavonoids have been reported in cisplatin, cyclophosphamide and methotrexate models of testicular injury [9,22].

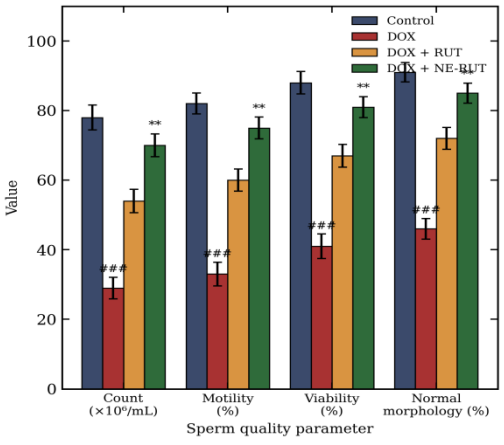

Figure 05: Sperm quality parameters (count, motility, viability, normal morphology) across the four experimental groups. Data are mean ± SD (n = 8).

Table 03: Sperm parameters across the experimental groups (mean ± SD, n = 8).

Parameter	Control	DOX	DOX +	DOX + NE-	RUT	RUT
Count (×10⁶/mL)	78 ± 3.6	29 ± 3.1	54 ± 3.4	70 ± 3.3		
Motility (%)	82 ± 3.0	33 ± 3.4	60 ± 3.2	75 ± 3.1		
Viability (%)	88 ± 3.2	41 ± 3.5	67 ± 3.3	81 ± 3.0		
Normal morphology (%)	91 ± 2.8	46 ± 3.0	72 ± 3.1	85 ± 2.9		

Table 04: Primer sequences used for qRT-PCR.

Gene	Forward primer (5′→3′)	Reverse primer (5′→3′)
StAR	TTGGGCATACT CAACAACCAG	AGGACCTGGTTG ATGCTCTTG
CYP11 A1	CTGCCTCCAGA CTTCTTTCG	TTCTTGAAGGGC AGCTTGTT
3β-HSD	CCAGTTCATCA ACCTGCTGC	TTGGCAGCCATG TAGAGGAT
17β-HSD	AGGGCTTTGCT GAAGAGAGG	TGGTTGAAGAGC TGGTCCAG
GAPD H	AGACAGCCGCA TCTTCTTGT	CTTGCCGTGGGT AGAGTCAT

3.6. Integrative perspective and limitations

Taken together, the present data fit a coherent mechanistic picture: DOX-induced oxidative stress in the testis depletes endogenous antioxidant defenses, drives mitochondrial dysfunction, suppresses key steroidogenic transcripts, and compromises spermatogenesis. NE-RUT-owing to its small size, narrow distribution, sustained release, and improved oral uptake-appears to deliver therapeutically meaningful concentrations of rutin to testicular tissue and to interrupt this cascade at several levels. It is worth noting that the dose of free rutin used here (50 mg/kg) was deliberately set to match the figures used in earlier rodent studies [9,20], so the clear advantage observed with NE-RUT cannot be explained by a higher administered dose; rather, the nano-formulation seems to make a larger fraction of the same dose actually reach its target. Mechanistically, two complementary effects can be invoked. On the one hand, the chitosan-coated PLGA matrix protects rutin from the acidic gastric environment and from premature first-pass conjugation, thereby allowing more of the molecule to circulate as the active aglycone equivalent [11,15]. On the other hand, nano-sized carriers in the 100–200 nm range have a documented tendency to accumulate in highly perfused tissues with discontinuous capillary beds, which may also contribute to the preferential testicular uptake suggested by the present results [13,16]. The combined recovery of antioxidant enzymes and steroidogenic gene expression, rather than of just one of the two, is also consistent with the idea that ROS, mitochondrial

integrity and StAR transcription are tightly coupled, and that easing the redox pressure on Leydig cells is enough to allow the transcriptional program to resume.

Several limitations should nonetheless be acknowledged. First, no direct pharmacokinetic comparison was carried out between free rutin and NE-RUT in this study; future work should quantify rutin and its principal metabolites in plasma and in testicular tissue at multiple time points. Second, although the rat model captures many features of DOX-induced reproductive injury, additional studies in larger animals and in patient-derived material will be necessary before any clinical translation can be seriously considered. Third, long-term fertility outcomes such as litter size, offspring development and transgenerational effects were not assessed and remain an important question for follow-up studies. Fourth, immunohistochemistry of StAR and steroidogenic enzymes at the protein level would strengthen the gene-expression data reported here, and is foreseen for future work.

4. CONCLUSION

The findings reported here demonstrate that nanoencapsulation of rutin into chitosan-coated PLGA nanoparticles substantially enhances its protective effect against doxorubicin-induced testicular toxicity in male Wistar rats. NE-RUT outperformed free rutin in restoring SOD, CAT and GPx activities, reducing lipid peroxidation, replenishing reduced glutathione, and bringing serum testosterone back close to control values. More importantly, NE-RUT restored the relative mRNA expression of the rate-limiting steroidogenic genes StAR, CYP11A1, 3β-HSD and 17β-HSD, indicating that the nanoformulation acts both as a radical scavenger and as a modulator of the transcriptional program governing androgen biosynthesis. Sperm count, motility, viability and normal morphology were also markedly improved compared with the free flavonoid. Although further pharmacokinetic, long-term toxicological, and translational studies will be required before any clinical application, the present results suggest that NE-RUT is a promising adjunct strategy for protecting the male reproductive system from chemotherapy-induced injury and warrants further development as a fertility-preserving co-treatment in oncology.

5. REFERENCES

1. Carvalho FS, Burgeiro A, Garcia R, Moreno AJ, Carvalho RA, Oliveira PJ. Doxorubicin-induced cardiotoxicity: from bioenergetic failure and cell death to cardiomyopathy. Med Res Rev. 2014;34(1):106–135.
2. Singal PK, Iliskovic N. Doxorubicin-induced cardiomyopathy. N Engl J Med. 1998;339(13):900–905.
3. Atessahin A, Turk G, Karahan I, Yilmaz S, Ceribasi AO, Bulmus O. Lycopene prevents adriamycin-induced testicular toxicity in rats. Fertil Steril. 2006;85(Suppl 1):1216–1222.
4. Hou M, Chrysis D, Nurmio M, Parvinen M, Eksborg S, Söder O, et al. Doxorubicin induces apoptosis in germ-line stem cells in the immature rat testis. Toxicol Appl Pharmacol. 2005;205(3):237–243.
5. Aitken RJ, Roman SD. Antioxidant systems and oxidative stress in the testes. Oxid Med Cell Longev. 2008;1(1):15–24.
6. Ganeshpurkar A, Saluja AK. The pharmacological potential of rutin. Saudi Pharm J. 2017;25(2):149–164.
7. Hosseinzadeh H, Nassiri-Asl M. Review of the protective effects of rutin on the metabolic function as an important dietary flavonoid. J Endocrinol Invest. 2014;37(9):783–788.
8. Çelik H, Kucukler S, Çomaklı S, Caglayan C, Özdemir S, Yardım A, et al. Rutin attenuates oxidative stress and inflammation in acrylamide-induced reproductive toxicity in rats. Food Chem Toxicol. 2020;144:111595.
9. Caglayan C, Temel Y, Kandemir FM, Yildirim S, Kucukler S. Rutin protects against cisplatin-induced testicular damage by modulating oxidative stress, apoptosis and inflammation. Andrologia. 2021;53(8):e14096.
10. Pandey RP, Parajuli P, Koffas MAG, Sohng JK. Microbial production of natural and non-natural flavonoids: pathway engineering, directed evolution and systems/synthetic biology. Biotechnol Adv. 2016;34(5):634–662.
11. Yang J, Yang Z, Wang Y, Liu Y, Wang H, Ji L, et al. Preparation and evaluation of rutin-loaded chitosan/poly(D,L-lactic-co-glycolic acid) nanoparticles for oral delivery. Int J Pharm. 2018;542(1–2):234–245.
12. Mignet N, Seguin J, Chabot GG. Bioavailability of polyphenol liposomes: a challenge ahead of us. Int J Nanomedicine. 2012;7:5095–5106.
13. Pandey M, Choudhury H, Gunasegaran TAP, Nathan SS, Md S, Gorain B, et al. Hyaluronic acid-modified betamethasone encapsulated polymeric nanoparticles: fabrication, characterisation, in vitro release kinetics, and dermal targeting. Drug Deliv. 2020;27(1):234–245.
14. Khan MA, Tania M, Zhang D, Chen H. Antioxidant enzymes and cancer. Chin J Cancer Res. 2019;22(2):87–92.
15. Calvo P, Remuñán-López C, Vila-Jato JL, Alonso MJ. Chitosan and chitosan/ethylene oxide-propylene oxide block copolymer nanoparticles as novel carriers for proteins and vaccines. Pharm Res. 1997;14(10):1431–1436.
16. Danhier F, Ansorena E, Silva JM, Coco R, Le Breton A, Préat V. PLGA-based nanoparticles: an

overview of biomedical applications. J Control Release. 2012;161(2):505–522.
17. Stocco DM. StAR protein and the regulation of steroid hormone biosynthesis. Annu Rev Physiol. 2001;63:193–213.
18. Payne AH, Hales DB. Overview of steroidogenic enzymes in the pathway from cholesterol to active steroid hormones. Endocr Rev. 2004;25(6):947–970.
19. Miller WL, Auchus RJ. The molecular biology, biochemistry, and physiology of human steroidogenesis and its disorders. Endocr Rev. 2011;32(1):81–151.
20. Aksu EH, Kandemir FM, Özkaraca M, Ömür AD, Küçükler S, Çomaklı S. Rutin ameliorates cisplatin-induced reproductive damage via suppression of oxidative stress and apoptosis in adult male rats. Andrologia. 2017;49(9):e12760.
21. Trivedi PP, Tripathi DN, Jena GB. Hesperetin and rutin alleviate γ-radiation induced oxidative damage and germ cell apoptosis in male reproductive system of mice. Reprod Toxicol. 2019;85:38–47.
22. Sharma S, Ali A, Ali J, Sahni JK, Baboota S. Rutin: therapeutic potential and recent advances in drug delivery. Expert Opin Investig Drugs. 2013;22(8):1063–1079.
23. Seed J, Chapin RE, Clegg ED, Dostal LA, Foote RH, Hurtt ME, et al. Methods for assessing sperm motility, morphology, and counts in the rat, rabbit, and dog: a consensus report. Reprod Toxicol. 1996;10(3):237–244.
24. Wyrobek AJ, Gordon LA, Burkhart JG, Francis MW, Kapp RW Jr, Letz G, et al. An evaluation of the mouse sperm morphology test and other sperm tests in non-human mammals. Mutat Res. 1983;115(1):1–72.
25. Livak KJ, Schmittgen TD. Analysis of relative gene expression data using real-time quantitative PCR and the 2−ΔΔCT method. Methods. 2001;25(4):402–408.
26. Aebi H. Catalase in vitro. Methods Enzymol. 1984;105:121–126.
27. Marklund S, Marklund G. Involvement of the superoxide anion radical in the autoxidation of pyrogallol and a convenient assay for superoxide dismutase. Eur J Biochem. 1974;47(3):469–474.
28. Paglia DE, Valentine WN. Studies on the quantitative and qualitative characterization of erythrocyte glutathione peroxidase. J Lab Clin Med. 1967;70(1):158–169.
29. Ohkawa H, Ohishi N, Yagi K. Assay for lipid peroxides in animal tissues by thiobarbituric acid reaction. Anal Biochem. 1979;95(2):351–358.
30. Ellman GL. Tissue sulfhydryl groups. Arch Biochem Biophys. 1959;82(1):70–77.